The glutamate/aspartate transporter EAAT1 is crucial for T-cell acute lymphoblastic leukemia proliferation and survival

Vesna S. Stanulović,[1] Shorog Al Omair,[1] Michelle A.C. Reed,[1] Jennie Roberts,[1] Sandeep Potluri,[1] Taylor Fulton-Ward,[2] Nancy Gudgeon,[2] Emma L. Bishop,[2] Juliette Roels,[3] Tracey A. Perry,[1] Sovan Sarkar,[1] Guy Pratt,[1,4] Tom Taghon,[3] Sarah Dimeloe,[2] Ulrich L. Günther,[1] Christian Ludwig[5] and Maarten Hoogenkamp[1]

[1]Institute of Cancer and Genomic Sciences, University of Birmingham, Birmingham, UK; [2]Institute of Immunology and Immunotherapy, University of Birmingham, Birmingham, UK; [3]Department of Diagnostic Sciences, Ghent University, Ghent, Belgium; [4]Center for Clinical Hematology, Queen Elizabeth Hospital Birmingham, Birmingham, UK and [5]Institute of Metabolism and Systems Research, University of Birmingham, Birmingham, UK

Correspondence: M. Hoogenkamp
m.hoogenkamp@bham.ac.uk

Received: May 3, 2023.
Accepted: May 20, 2024.
Early view: May 30, 2024.

https://doi.org/10.3324/haematol.2023.283471

Figure S1

	ARR (T I/ETP)	DU.528 (T II)	HSB2 (T III)	CCRF-CEM (T IV)	Molt-4 (T III)	Jurkat (T IV)
CD34	+	-	-	-	+	-
CD7	+	+	+	+	+	+
CD5	-	+	+	+	+	+
CD1a	-	-	+	+	+	+
CD3	-	-	-	+	-	+
CD4	-	-	-	+	+	+
CD8	-	-	-	-	+	-

Figure S2

A

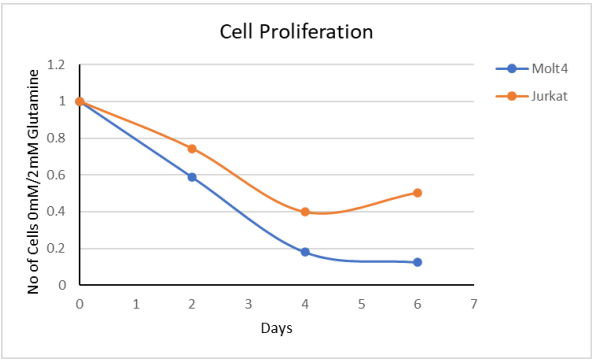

B

	Oncogenic subtype	Notch1 Mutation
ARR	ETP	-
DU.528	TAL	WT
HSB2	TAL	WT
CCRF-CEM	TAL	Mut
Molt-4	TAL	Mut
Jurkat	TAL	Mut

Figure S3

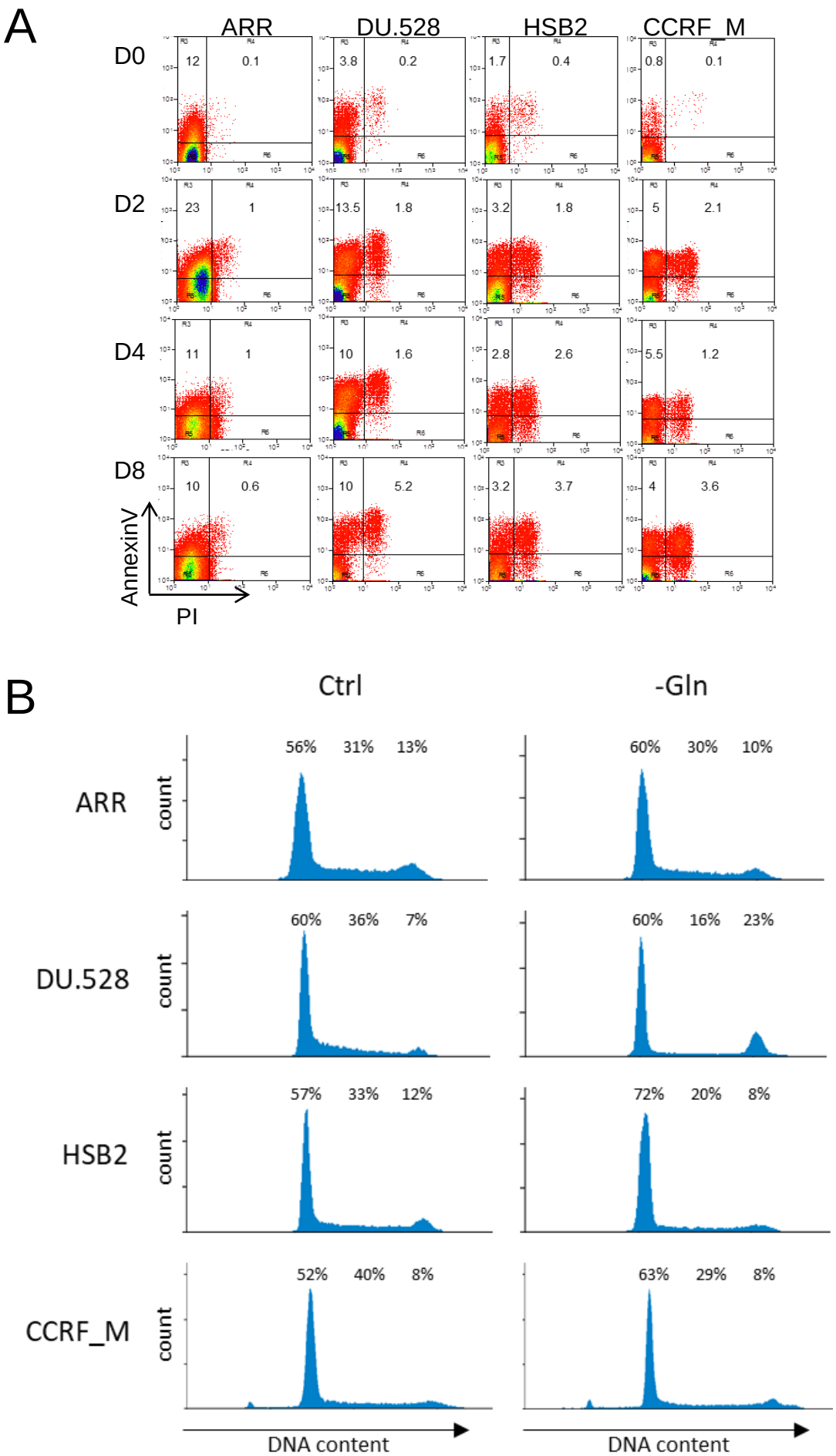
A
ARR
DU.528
HSB2
CCRF_M
D0
D2
D4
D8
12
0.1
3.8
0.2
1.7
0.4
0.8
0.1
23
1
13.5
1.8
3.2
1.8
5
2.1
11
1
10
1.6
2.8
2.6
5.5
1.2
10
0.6
10
5.2
3.2
3.7
4
3.6
AnnexinV
PI
B
Ctrl
-Gln
ARR
DU.528
HSB2
CCRF_M
count
56%
31%
13%
60%
30%
10%
60%
36%
7%
60%
16%
23%
57%
33%
12%
72%
20%
8%
52%
40%
8%
63%
29%
8%
DNA content
DNA content

Figure S4

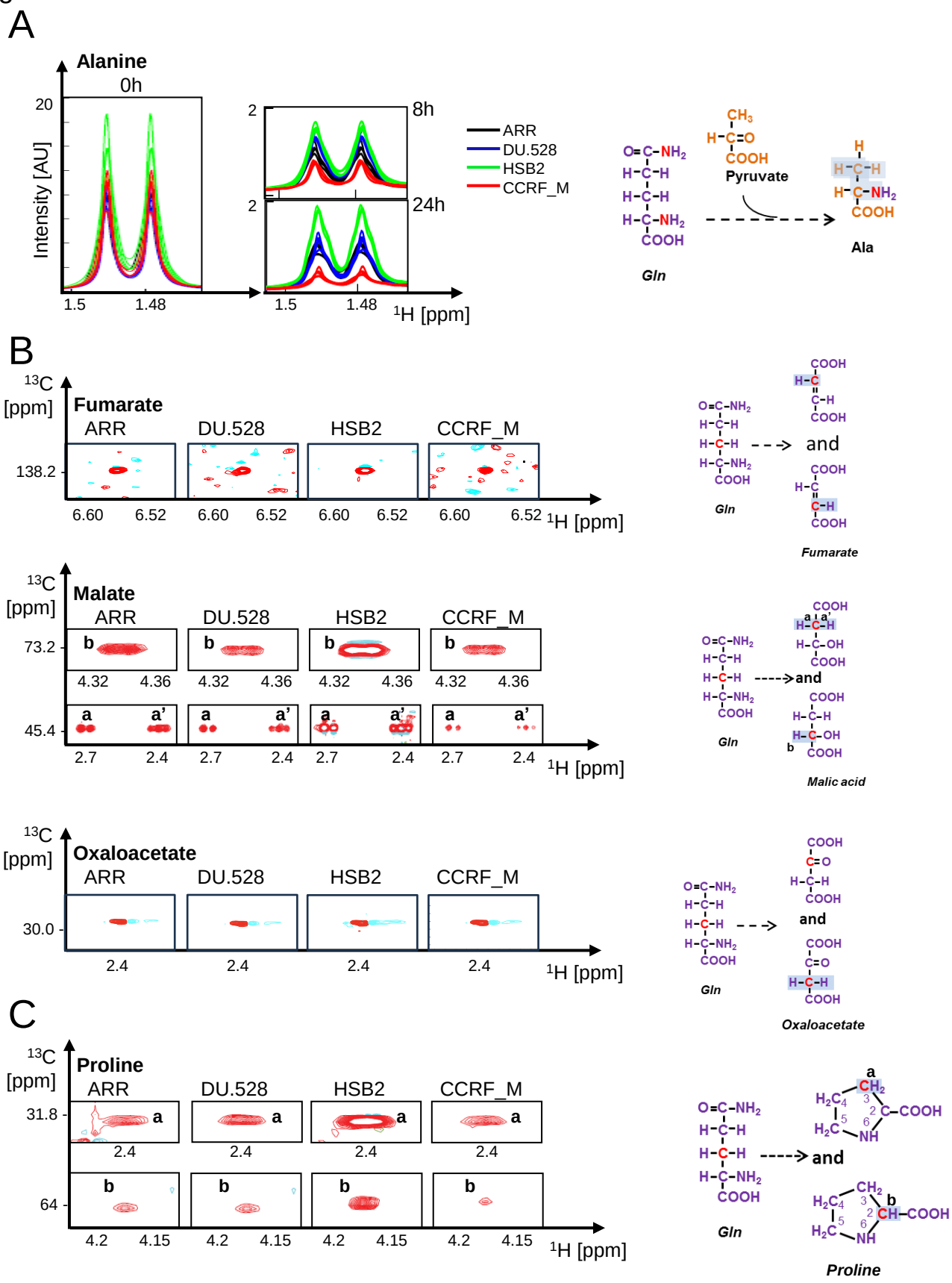
A
Alanine
0h
8h
24h
Intensity [AU]
ARR
DU.528
HSB2
CCRF_M
1.5
1.48
1H [ppm]
Pyruvate
Gln
Ala
B
13C [ppm]
Fumarate
138.2
6.60
6.52
and
Malate
73.2
45.4
4.32
4.36
2.7
2.4
Malic acid
Oxaloacetate
30.0
C
Proline
31.8
64
4.2
4.15

Figure S5

SLC1A3 expression

	patients (% of all)				patients (Nº)				
FPKM	0	low (<0.1)	medium (0.1-1)	high (>1)	FPKM	0	low (<0.1)	medium (0.1-1)	high (>1)
SLC1A3	3	50	32	14	SLC1A3	9	133	85	37

maturation stage

	0	low (<0.1)	medium (0.1-1)	high (>1)		0	low (<0.1)	medium (0.1-1)	high (>1)
pre-cortical	**10**	50	35	5	pre-cortical	4	20	14	2
cortical	1	53	29	17	cortical	2	83	46	26
post-cortical	8	40	44	8	post-cortical	2	10	11	2
N/A	3	46	31	21	N/A	1	18	12	8

oncogenic subtype

	0	low (<0.1)	medium (0.1-1)	high (>1)		0	low (<0.1)	medium (0.1-1)	high (>1)
HoxA	6	73	**18**	3	HoxA	**2**	**24**	**6**	**1**
LMO1/2	11	**25**	**54**	11	LMO1/2	**3**	**7**	**15**	**3**
NKX2_1	0	**86**	**14**	0	NKX2_1	0	12	2	0
TAL1/2	0	35	32	**34**	TAL1/2	**0**	**33**	**30**	**32**
TLX1/3	4	55	38	3	TLX1/3	**3**	**43**	**30**	**2**
unknown	5	62	29	5	unknown	1	13	6	1

ETP status

	0	low (<0.1)	medium (0.1-1)	high (>1)		0	low (<0.1)	medium (0.1-1)	high (>1)
ETP	11	**28**	39	**22**	ETP	2	5	7	4
near ETP	4	38	25	**33**	near ETP	1	9	6	8
not ETP	3	58	31	**9**	not ETP	4	84	45	13
N/A	3	45	34	18	N/A	2	33	25	13

Notch mutations

	0	low (<0.1)	medium (0.1-1)	high (>1)		0	low (<0.1)	medium (0.1-1)	high (>1)
mutated	4	56	32	**8**	mutated	7	110	63	15

Figure S6

A

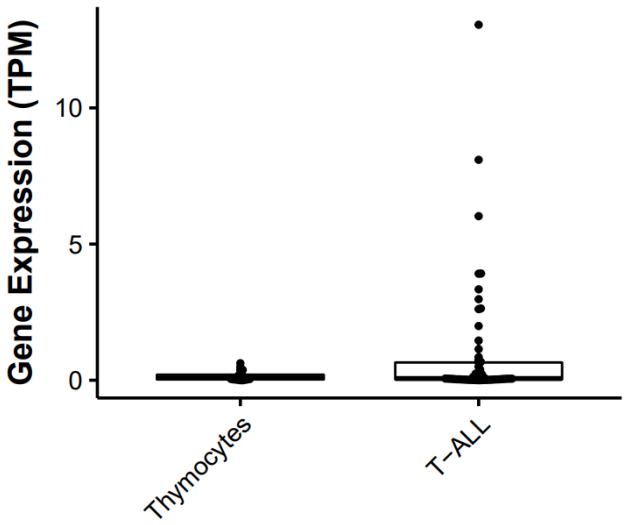
SLC1A3 Expression
Gene Expression (TPM)
10
5
0
Thymocytes
T−ALL

B

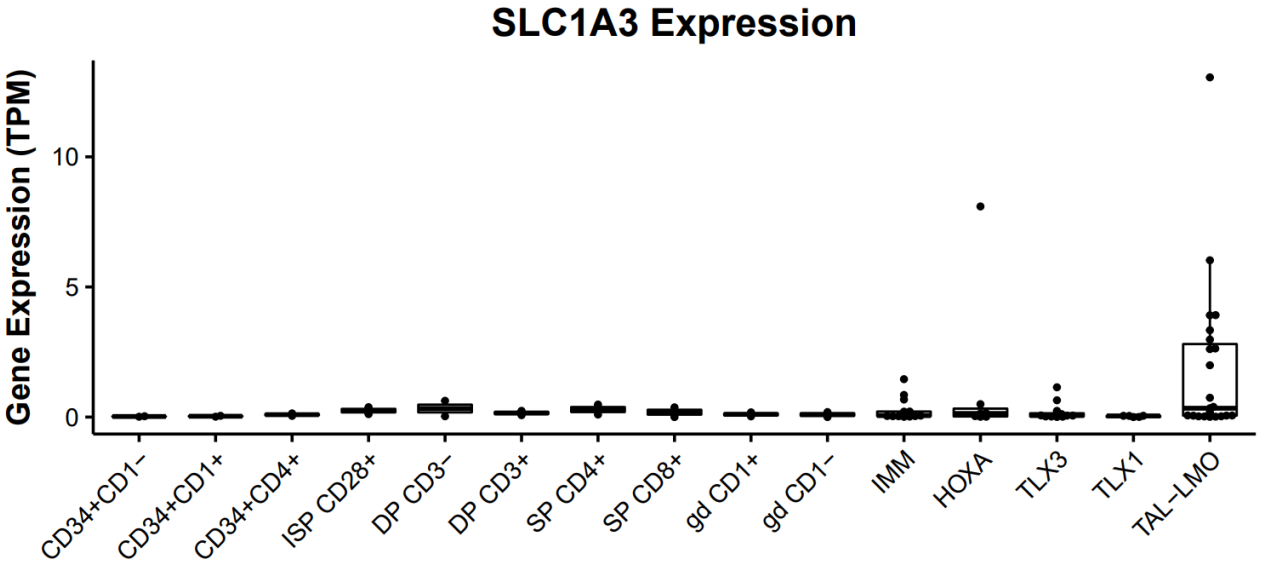
SLC1A3 Expression
Gene Expression (TPM)
10
5
0
CD34+CD1−
CD34+CD1+
CD34+CD4+
ISP CD28+
DP CD3−
DP CD3+
SP CD4+
SP CD8+
gd CD1+
gd CD1−
IMM
HOXA
TLX3
TLX1
TAL−LMO

Figure S7

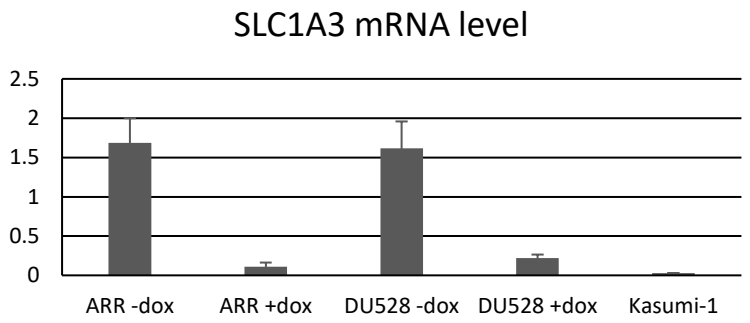

Figure S8

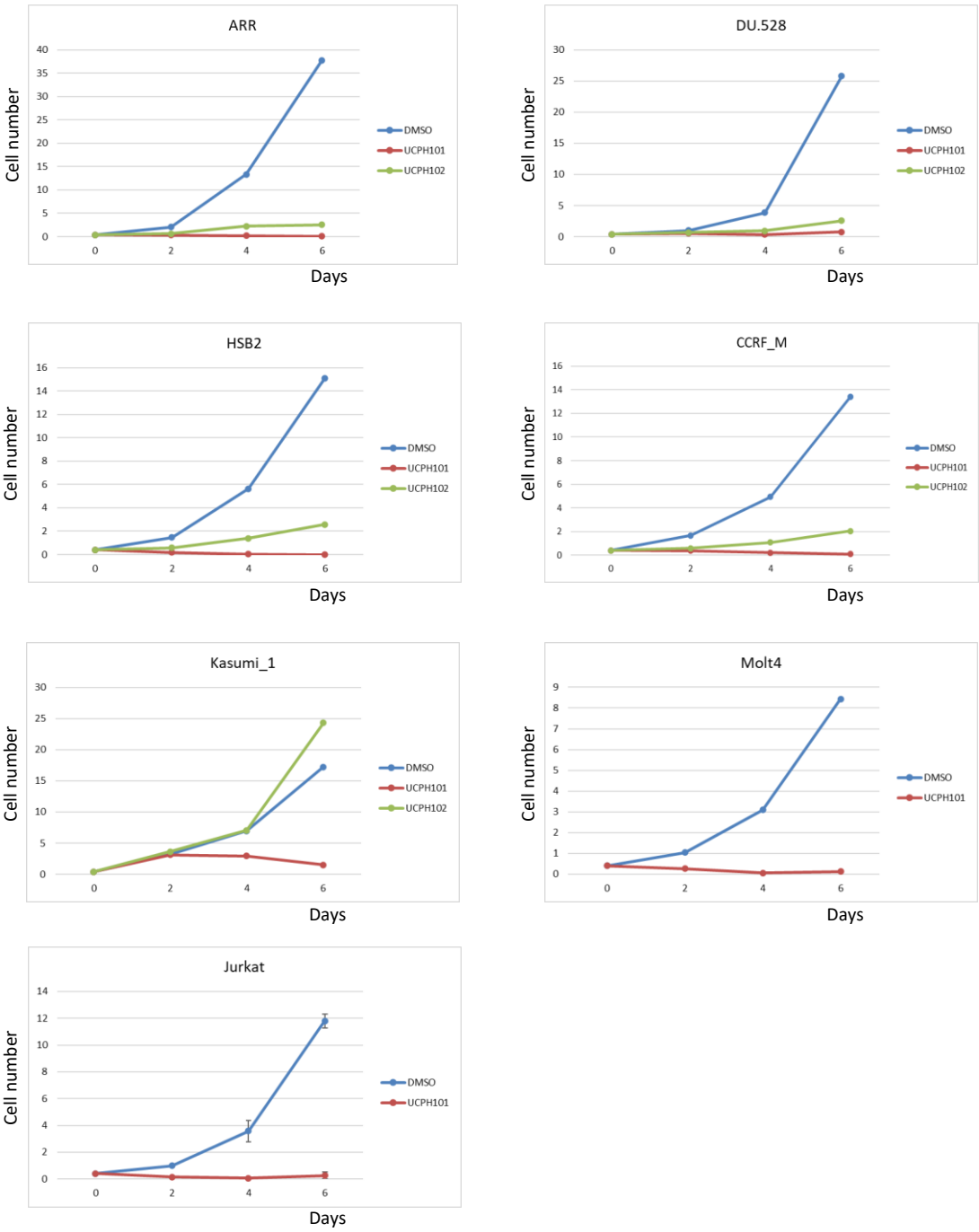

Figure S9

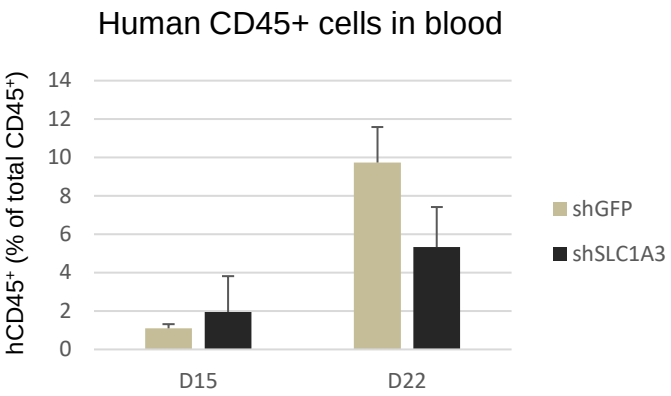
Human CD45+ cells in blood
hCD45+ (% of total CD45+)
14
12
10
8
6
4
2
0
D15
D22
shGFP
shSLC1A3

Supplemental Figure Legends

Figure S1. Immunophenotypes of the T-ALL cell lines, with their EGIL classification, used within this study Sandberg *et al.* (2007).

Figure S2. A) Molt-4 and Jurkat cell lines were cultured in medium with 10% FCS, with or without 2mM GlutaMax. Four independent cell cultures were assayed per cell line and each point represents the mean ± StDev. **B)** Indication of oncogenic subgroup and Notch1 mutation status for the T-ALL cell lines used within this study (Etchin et al., 2013).

Figure S3. A) Glutamine deprivation induces apoptosis in T-ALL cell lines. Scatter plots show flow-cytometry Annexin V and propidium iodide staining by flow-cytometry of cells grown in RPMI media supplemented with 10% FBS in the absence of glutamine. Gating was determined based on the staining of T-ALL cells grown in the RPMI media supplemented with 2mM glutamine. Cells were grown for the indicated number of days (D0-D8) prior to staining and analysis. **B)** Cell cycle analysis after removal of glutamine. Cells were cultured for 4 days in the absence of glutamine from the medium and analysed by flow cytometry after the addition of DAPI to the samples. Live cells were gated and percentages indicate cells in the G0/G1, S, and G2 phase of the cell cycle respectively.

Figure S4. Metabolite tracing experiments using [2,5-^{15}N]Glutamine and [3-^{13}C]Glutamine. T-ALL cell lines were grown in the presence of 2mM [2,5-^{15}N]Glutamine) (A) or [3-^{13}C]Glutamine) (B-D). **A)** Overlay of 1D ^{1}H-NMR spectra showing the Hβ-alanine resonance after 0, 8 and 24h and schematic representations of [2,5-^{15}N]Glutamine and the observed [2-^{15}N]Alanine. ^{15}N are in red and shading indicates the observed ^{3}J scalar couplings between the alanine Hβs and glutamine-derived ^{15}N. The X-axis shows the chemical shift relative to TMSP in ppm and the Y-axis indicates TSA scaled intensity. **B,C)** Resonances observed in ^{1}H-^{13}C-HSQC for T-ALL cells grown in the presence of [3-13C]Glutamine for 24h. Resonances are marked by letters **a-b**. Schematics on the right show fumarate, malate, oxaloacetate and proline with colour-coded atoms based on the substrate of their origin. Blue shaded lines indicate observed couplings.

Figure S5. Correlations between *SLC1A3* expression levels and maturations stage, oncogenic subtype, or ETP status of 265 patient samples, as reported by Liu *et al.* (2017). Data are grouped by the level of expression. The left tables show the percentage of patients within each group, whereas the right panels show absolute counts. Significant differences between the total distribution pattern of expression levels and those of different subgroups

were determined using a Chi-square test and are indicated by shading and bold numbers. Additionally, percentages that changed more than a factor 1.5 compared to the percentages in the top panel (*SLC1A3* expression), and were representative of more than 3 patient samples, are shown in green if raised and in red if reduced.

Figure S6. Comparison of *SLC1A3* expression levels between healthy T-cell progenitors and T-ALL patient samples. Published RNAseq data for ten healthy thymocyte progenitor subsets (Roels *et al.*, 2020) and sixty T-ALL patient samples (Verboom *et al.* 2018) were analyzed. **(A)** Overall comparison between the two data sets indicates a statistically significant difference ($p<0.05$). **(B)** The same data subdivided according to isolated T-cell progenitor stages and T-ALL oncogenic subtypes as determined in Verboom et al (2018). Purified thymocyte populations are: CD34+CD1- ($CD34^+CD1a^-CD4^-$), CD34+CD1+ ($CD34^+CD1a^+CD4^-$), CD34+CD4+ ($CD34^+CD1a^+CD4^+$), ISP CD4+CD28+ ($CD4^+CD34^-CD3^-CD8^-$HLA-DR^-CD28^+), DP CD3– ($CD4^+CD8^+CD3^-$), DP CD3+ ($CD4^+CD8^+CD3^+$), SP CD4+ ($CD4^+CD8^-CD3^+$), SP CD8+ ($CD4^-CD8^+CD3^+$), gd CD1a+ ($CD3^+$TCRγδ$^+CD1a^+$), gd CD1a– ($CD3^+$TCRγδ$^+CD1a^-$). IMM; immature oncogenic subgroup of T-ALL. TPM; transcripts per million.

Figure S7. SLC1A3 mRNA expression level in T-ALL cell lines ARR and DU.528, in the presence or absence of shSCL1A3 knockdown, and the AML cell line Kasumi-1. Expression was measured by qPCR and shown relative to rRNA level. Data are the average ± StDev.

Figure S8. The effect of EAAT1 inhibition on individual cell lines, compared to the vehicle control (DMSO). Cell lines were cultured for six days in the presence of vehicle (DMSO), 25 µM UCPH-101, or 25 µM UCPH-102. Each data point is an average of three or four independent measurements ± StDev.

Figure S9. Mice were injected (iv) with 3 x10^5 cells CCRF-CEM cells carrying doxycycline-inducible shSLC1A3_2 or shGFP. At day 16, the food was supplemented with doxycycline. The bar diagram shows the frequency of human $CD45^+$ cells in the two cohorts of mice (n=5) prior to (day 15) and after 6 days of doxycycline treatment (day 22).

Table S1.
List of Differentially expressed genes.

Table S2.
Gene functional annotation clusters identified for cluster C1 in Figure 1.

Table S3.

Gene functional annotation clusters identified for cluster C2 in Figure 1.

Table S4.

Gene lists of gene functional annotation clusters shown in Figure 1B.

Experimental Procedures

Cell Culture

T-ALL cell lines were grown in RPMI 1640medium (Merck) supplemented with 10% FCS, Pen/Strep, 2mM Glutamine or GlutaMax (LifeTechnologies) and 0.075mM 1-Thyoglycerol (Merck) in a humidified incubator at 37°C and 5% CO_2. Where indicated, 25μM UCPH-101 or UCPH-102 (Abcam) was added. For labelling experiments, glutamine-free RPMI was supplemented with 2mM [1,5-^{15}N]-L-Glutamine or [3-^{13}C]-L-Glutamine (Merck).

For *In vitro* differentiation of human T-cell progenitors, mononuclear cells were isolated from cord blood using Lymphoprep™ (StemCell Technologies); HBRC Application 15-224 under generic approval 15/NW/0079. Red blood cells were lysed with 1x Lysing buffer (BD Biosciences) and $CD34^+$ cells were isolated using a human CD34 MicroBead Kit (Miltenyi Biotec). $CD34^+$ cells were co-cultured on 80% confluent OP9-DL4 cells in αMEM medium, supplemented with 5 ng/ml human FLT3L (Peprotech) and 5 ng/ml human IL7 (Peprotech). Cells were sorted at specific time points for RNA isolation and subsequent RNA sequencing; day 7 for $CD7^+$,$CD5^-$,$CD1a^-$ cells, day 14 for $CD7^+$,$CD5^+$,$CD1a^-$ cells, and day 21 for $CD7^+$,$CD5^+$ $CD1a^+$,$CD3^-$ cells. Purification of cell populations was performed using a BD FACSAria Fusion (BD Biosciences) cell sorter.

CD4+ and CD8+ T cells were isolated using Miltenyi Microbeads (CD4 Cat#130-045-101, CD8 Cat#130-045-201) from mononuclear cells separated as above from leukocyte cones (NHS Blood and Transplant); University of Birmingham STEM Ethics ERN_17-1743. CD4+/CD8+ T cells were either left unstimulated or stimulated with Immunocult T cell activator (Stemcell Technologies Cat#10991) for 48 hours prior to snap freezing and RNA extraction.

Expression analysis

RNA isolation and cDNA synthesis was performed as previously described (Stanulovic et al 2017). Quantitative PCR (qPCR) was performed using an ABI 7500 Real-Time PCR System. Quantitation was carried out using a standard curve of serial dilutions and relative to rDNA. Primers used for quantification: SLC1A3F 5'AAGAGAACAATGGCGTGGAC, SLC1A3R 5'ATTCCAGCTGCCCCAATACT, 18SrRNAF 5'GGCCCGAAGCGTTTACTTTGA, 18SrRNAR 5'GAACCGCGGTCCTATTCCATTA.

RNASeq

RNASeq libraries were prepared and indexed using the TruSeq Stranded mRNA Sample Preparation Kit LH (Illumina) according to the manufacturer's protocol. Libraries were pooled and sequenced as 100 nt paired-end on Illumina HiSeq 2500 sequencer at a depth of approximately 30 million reads per library.

Reads acquired from RNASeq were mapped as stranded libraries to the human genome (GRCh38), using HISAT2 at usegalaxy.org[1,2]. Transcripts were assembled using StringTie and GENCODE gene annotation with quartile normalisation and effective length correction[3]. Duplicate biological replicates were used. Differential gene expression was determined by DESeq2 between T-ALL samples and $CD34^+$ hematopoietic progenitors and *in vitro* differentiated samples ($CD7^+$ $CD5^-$ $CD1a^-$, the $CD7^+$ $CD5^+$ $CD1a^-$, and the $CD7^+$ $CD5^+$ $CD1a^+$ $CD3^-$). Normalised gene counts of the significantly differentially expressed genes were used to select the gene IDs that were significantly differentially expressed. Pearson average linkage hierarchical clustering and heat maps were computed by Multi Experiment Viewer software[4]. Gene functional annotation clustering was performed using DAVID v2023q3[5,6]. Clusters with enriched terms with Modified Fisher Extract P-value <0.05 were considered significant, categories with redundant terms were filtered out. Data has been deposited at NCBI-GEO GSE101566.

Western blot analysis

Cell extracts were prepared by lysing cells in RIPA buffer (50mM TRIS pH8, 150mM NaCl, 0.5% deoxycholic acid, 1% NP40, 0.1% SDS) on ice for 20 min. The insoluble fraction was precipitated by centrifuging at 20,000 g for 10min. Protease inhibitor and PhosSTOP (Roche) were used 1:100.

Proteins were separated on 4-12% gradient Bis-Tris Plus Bolt Mini Gels (LifeTechnologies), transferred to nitrocellulose membranes and stained with PonceauS to confirm equal loading prior to o/n incubation with antibodies. Primary antibodies raised against EAAT1 (D4166; Cell Signalling) and GFP (GF28R; eBiosciences) were used at a final concentration of 1µg/ml. Secondary antibodies, IRDye 680RD or 800RD (Li-Cor), were used at a 0.5µg/ml. Westerns were visualised using an Odyssey CLx Imager (Li-Cor).

Immunofluorescent Staining

Cells were fixed with 2% formaldehyde for 10min and washed twice in PBS/0.05%Tween/2%FCS, followed by o/n incubation with 1µg/ml primary antibody. Cells were washed and incubated with 1µg/ml secondary antibody conjugated to Alexa dyes (LifeTechnologies). Immuno-stained cells were deposited onto the glass slides using a Cytospin III centrifuge (Shandon). MitoTracker Red CMXRos (Invitrogen) was used for mitochondria staining as per manufacturer's instruction. Slides were dried, covered with Prolong Gold Anti-Fade DAPI reagent (LifeTechnologies) and imaged using a Zeiss LSM880 Confocal microscope.

SLC1A3 knockdown

SLC1A3 was amplified by PCR from pcDNA3-EAAT1. The PCR product was cloned into MigR1 in front of IRES-GFP[7]. Short hairpin sequences targeting *SLC1A3* were designed using http://cancan.cshl.edu/RNAi_central/RNAi.cgi?type=shRNA[8]. Designed shRNA (shSLC1A3_1 ACCATATCAACTGATTGCACAG, shSLC1A3_2 GGGTAACTCAGTGATTGAAGAG, shSLC1A3_3 GTGGCACACAATCCTATAAATG ,shSLC1A3_4 AGGCCTCAGTGTCCTCATCTAT and shSLC1A3_5 CACTCCTCAACTGATGATAGAC) were embedded into mir30 and cloned into pMSCVhygro[9]. The mouse fibroblast cell line PlatE was transfected using *Trans*IT-LT1 (Mirusbio) with MigRI-SLC1A3 and MSCVhyg_shSLC1A3, MSCVhyg_shGFP, or MSCVhyg_shFF3[8,10].

Functional shRNA was cloned into piggybac transposon inducible expression vector PB_tet-on_Apple_shGFP using *Hind*III and *Kpn*2L (ThermoFisher)[11]. T-ALL cell lines were electroporated with pB_shSLC1A3 and p*CAGG-PBase* [12], expanded and selected with puromycin (ThermoFisher). Expression of shRNA was induced with 0.1µg/ml doxycycline (Merck). Cells were counted every other day and the cell concentration was adjusted to $0.4x10^6$/ml.

Patient Samples

The patients' cells used in this study were from diagnostic samples from presentation cases before treatment. They were obtained from the Queen Elizabeth Hospital Birmingham, Birmingham, UK with ethical approval from the NHS National Research Ethics Committee (Reg:10/H1206/58). Cytogenetic abnormalities and sample immunophenotype were determined at the time of disease diagnosis at the West Midlands Regional Genetics Laboratory, Birmingham Women's NHS Foundation Trust, Birmingham, UK.

Mononuclear cells were purified from peripheral blood by differential centrifugation using Lymphoprep (Axis-Shield UK). Undifferentiated blast cells were isolated using anti-human CD34 (T-ALL_1 and _2) or CD7 (T-ALL_3) MACS microbeads (Miltenyi). For T-ALL_2, $CD34^+$ cells were further sorted by FACS for $CD7^+$ using anti-human CD7-FITC antibody (CD6-6B7; BioLegend).

Intracellular NMR spectroscopy

Methanol/chloroform extraction was used to prepare polar extracts from $5x10^7$ cells. Following centrifugation, the polar phase was dried in a vacuum concentrator. Pellets were resuspended in 50µl NMR buffer (100 mM sodium phosphate pH7.0, 500µM Sodium 3-(trimethylsilyl)propionate (TMSP; Merck), 10% D_2O) and transferred to 1.7mm NMR tubes. NOESY 1D spectra with water pre-saturation were acquired using the standard Bruker pulse sequence noesygppr1d on a Bruker 600MHz spectrometer with a TCI 1.7mm z-PFG

CryoProbe™. The sample temperature was set to 300K. The ^{1}H carrier was on the water frequency and the ^{1}H 90° pulse was calibrated at a power of 0.326W. Key parameters were: spectral width 12.15ppm/7288.6Hz; complex data points, 16384; interscan relaxation delay, 4s; acquisition time, 2.25s; short NOE mixing time, 10ms; number of transients, 256; steady state scans, 4.

Growth-media metabolite uptake and release

Growth medium was collected and supplemented with 10% D_2O and 1mM TMSP. Samples were transferred to 5mm glass NMR tubes and spectra were acquired at 300K, using a Bruker 500 MHz spectrometer equipped with a TXI probe. The ^{1}H carrier was on the water frequency and the ^{1}H 90° pulse was calibrated at a power of 12.9W. Measurements were carried out after locking on deuterium frequency and shimming. The standard Bruker 1D NOESY pulse sequence (noesygppr1d) with water saturation was used. Spectra were acquired with 64 transients and 4 steady state scans.

Live-cell real-time NMR spectroscopy

Cells were resuspended at 10^{6}/ml growth media containing 0.1% low melting agarose (Sigma), 1mM TMSP, 10% D_2O. Samples were loaded into 5mm NMR tubes and measurements were collected every 8.4 minutes, for a total of 100 time points. CPMG (Carr-Purcell-Meiboom-Gill) 1D spectra with water pre-saturation were acquired using the standard Bruker pulse sequence cpmgpr1d on a Bruker 500 MHz spectrometer with a TXI ^{1}H/D-^{13}C/^{15}N probe at 310K. The ^{1}H carrier was on the water frequency and the ^{1}H 90° pulse was calibrated at a power of 12.9W. For the CPMG T_2 filter, a T_2 filter time of 68 ms arose from 100 loops over a 680 µs echo time between 180 pulses. Other key parameters were: spectral width 12.02 ppm/6009.6 Hz; complex data points, 16384; interscan relaxation delay, 4s; acquisition time, 2.73s; short NOE mixing time, 10ms; number of transients, 64; steady state scans, 4.

NMR spectroscopy data processing and analysis

NMR spectroscopy data was processed in Topspin (Bruker Ltd, UK), MetaboLab (version 20910688) in MATLAB (version R2015b)[13] and MetaboLabPy (https://pypi.org/project/qtmetabolabpy). All spectra were aligned to TMSP, a spline baseline correction was applied, the water and TMSP regions were excluded, and the total spectral area (TSA) of each spectrum was scaled to 1. To compare metabolite concentrations, a well-resolved peak was picked for each metabolite in the first spectrum and peaks were picked in the other spectra in an automated manner using in-house subroutines of MetaboLab (version 20910688). Spectral assignments were made using Chenomx software and acquired chemical standards.

Mouse studies

Animal experiments were performed at the University of Birmingham Biomedical Services Unit under an animal project licence (PP8841933) in accordance with UK legislation. Female NOD.Cg-Prkdcscid Il2rgtm1Wjl/SzJ (NSG) mice aged 8-9 weeks at study commencement were used for the xenograft model. CCRF-CEM cells were transfected with pBshSLC1A3_2 or pBshGFP control vector and pCAGG-PBase as described above. After selection, $3x10^5$ cells per mouse were injected *intra venous* using the tail vein. When approximately 1% engraftment was observed, the next day all animals were transferred to a diet supplemented with 0.625g/kg doxycycline hyclate.

References

1. Afgan E, Baker D, Batut B, et al. The Galaxy platform for accessible, reproducible and collaborative biomedical analyses: 2018 update. *Nucleic Acids Res*. 2018;46(W1):W537-W544.
2. Kim D, Langmead B, Salzberg SL. HISAT: a fast spliced aligner with low memory requirements. *Nat Methods*. 2015;12(4):357-360.
3. Pertea M, Pertea GM, Antonescu CM, Chang TC, Mendell JT, Salzberg SL. StringTie enables improved reconstruction of a transcriptome from RNA-seq reads. *Nat Biotechnol*. 2015;33(3):290-295.
4. Howe EA, Sinha R, Schlauch D, Quackenbush J. RNA-Seq analysis in MeV. *Bioinformatics*. 2011;27(22):3209-3210.
5. Huang da W, Sherman BT, Lempicki RA. Systematic and integrative analysis of large gene lists using DAVID bioinformatics resources. *Nat Protoc*. 2009;4(1):44-57.
6. Huang da W, Sherman BT, Lempicki RA. Bioinformatics enrichment tools: paths toward the comprehensive functional analysis of large gene lists. *Nucleic Acids Res*. 2009;37(1):1-13.
7. Pear WS, Miller JP, Xu L, et al. Efficient and rapid induction of a chronic myelogenous leukemia-like myeloproliferative disease in mice receiving P210 bcr/abl-transduced bone marrow. *Blood*. 1998;92(10):3780-3792.
8. Paddison PJ, Cleary M, Silva JM, et al. Cloning of short hairpin RNAs for gene knockdown in mammalian cells. *Nat Methods*. 2004;1(2):163-167.
9. Dow LE, Premsrirut PK, Zuber J, et al. A pipeline for the generation of shRNA transgenic mice. *Nat Protoc*. 2012;7(2):374-393.
10. Morita S, Kojima T, Kitamura T. Plat-E: an efficient and stable system for transient packaging of retroviruses. *Gene Ther*. 2000;7(12):1063-1066.
11. Glover JD, Taylor L, Sherman A, Zeiger-Poli C, Sang HM, McGrew MJ. A novel piggyBac transposon inducible expression system identifies a role for AKT signalling in primordial germ cell migration. *PLoS One*. 2013;8(11):e77222.
12. Wang W, Lin C, Lu D, et al. Chromosomal transposition of PiggyBac in mouse embryonic stem cells. *Proc Natl Acad Sci U S A*. 2008;105(27):9290-9295.
13. Ludwig C, Gunther UL. MetaboLab--advanced NMR data processing and analysis for metabolomics. *BMC Bioinformatics*. 2011;12:366.